European Review for Medical and Pharmacological Sciences 2020; 24: 1515-1523

Bone marrow mesenchymal stem cells repair brachial plexus injury in rabbits through ERK pathway

M.-G. GUO, D.-P. LI, L.-X. WU, M. LI, B. YANG

Department of Neurosurgery, The First Affiliated Hospital of Zhengzhou University, Zhengzhou, China

Abstract. – OBJECTIVE: To investigate the effect of bone marrow mesenchymal stem cells (BMSCs) on repairing brachial plexus injury in rabbits and their influence on expression of the extracellular signal-regulated kinase (ERK) pathway.

MATERIALS AND METHODS: With big-ear rabbits as the objects, the BMSCs were first isolated, and the cluster of differentiation (CD)45$^-$ and CD90$^+$ BMSCs were sorted out *via* flow cytometry. BMSCs were transfected with red fluorescent protein (RFP), and the transfection effect was detected. Then, the big-ear rabbits were subjected to brachial plexus root avulsion injury (BPAI) to establish injury Model group and sham-operation group (Sham group). Later, the BMSCs were transfected with RFP to construct RFP-BMSCs. The RFP-BMSCs (5×10^6, Treat group) and normal saline (Model group) were intraperitoneally injected, and the recovery rate of wet weight of the upper limb muscle was measured by weighing. The injured nerve tissues were embedded for hematoxylin and eosin (HE) staining and observation of pathological changes. The electrophysiological measurement of the compound muscle action potential (CMAP) on the injured side was conducted for the rabbits to be sacrificed immediately using an electromyogram instrument, and the CMAP amplitude and latency were applied to evaluate the recovery of upper limb muscle. Finally, the location of RFP-BMSCs in the nerve tissues was traced by a fluorescence microscope, and the protein expression levels of phosphorylated ERK (p-ERK) and phosphorylated mitogen-activated protein kinase (p-MAPK) in the injured nerve tissues were determined by means of Western blotting.

RESULTS: Persistently expressed red fluorescence was observed in CD45- and CD90+ BMSCs sorted via flow cytometry under the fluorescence microscope, indicating that the RFP-BMSCs were constructed successfully. Compared with Sham group, Model group had a remarkably decreased recovery rate of wet muscle weight ($p<0.05$), while Treat group exhibited a notably increased recovery rate of wet muscle weight in comparison with Model group. The CMAP amplitude was reduced markedly ($p<0.05$), while the CMAP latency was prolonged significantly ($p<0.05$) in Model group compared with those in Sham group. Moreover, Treat group had distinctly higher CMAP amplitude and evidently shorter CMAP latency than Model group ($p<0.05$). It was discovered under the fluorescence microscope that RFP-BMSCs were visibly arranged on both sides of nerve fibers in Treat group. The expressions of p-MAPK and p-ERK were raised prominently in Model group in comparison with those in Sham group ($p<0.05$), and they were lowered apparently in Treat group compared with those in Model group ($p<0.05$).

CONCLUSIONS: BMSCs can repair the impaired brachial plexus neurons and restore their physiological functions, and the protective effect of the BMSCs on the neurons is associated with the mediated MAPK/ERK pathway.

Key Words:
Bone marrow mesenchymal stem cells, Brachial plexus root avulsion injury, MAPK/ERK.

Introduction

Recovering limb functions is the major task of treating peripheral nerve injury. It has been reported that nerve damage affects 2.8% of patients with trauma[1]. The injury ranges from nerve compression to complete nerve transection, and breakpoints appear in the neural structure at the involved site, without continuity. Under such circumstances, re-anastomosis is the only reliable therapeutic method. Trauma can influence the sciatic nerve, femoral nerve, facial nerve, and other peripheral nerves, thus causing corresponding regional paralysis. The characteristics of neural injury, a common peripheral neuropathy, are muscle weakness, reflection change, and numbness. Most patients will have persistent pain, dyskinesia, and even long-term disability[2]. The biggest problem of restoring the neurological function is the slow growth of neurites, thereby delaying re-innervation

Corresponding Author: Bo Yang, MD; e-mail: yang0bo62@163.com

of muscles[3]. In spite of progress in nerve fascicle or fascicular suture, the outcome of tension-free nerve repair is not the optimum, which may be attributed to internal and external factors of the nervous system[4]. Several alternative traditional therapeutic methods are under investigation, among which stem cell transplantation has attracted much attention[5-9].

Mesenchymal stem cells (MSCs) are able to renew themselves and differentiate into multiple lineages, including neuronal cells (e.g., Schwann cells), which can enhance neural regeneration through the MSCs[10,11]. The therapeutic benefit of MSCs in animal models of such brain diseases as Parkinson's disease, multiple sclerosis, stroke, brain injury, spinal cord injury, and peripheral nerve injury has been displayed[12-15]. MSCs possess the potential of inducing myogenesis and angiogenesis by releasing different angiogenic, mitogenic, and anti-apoptotic factors, including vascular endothelial growth factor (VEGF), IGF-1, HGF, and Bcl-2[16]. In addition, MSCs produce other paracrine factors, such as stem cell factor and heat-shock protein 20, that participate in remodeling, regeneration, and neovascularization, thus improving organ functions[16]. In the existence of paracrine factors VEGF, TGF-β1, and NO, MSCs are capable of ameliorating the blood flow in rat model of hindlimb ischemia[17]. Moreover, they have the unique capacity to migrate to the regions with hypoxia and tissue injury and strengthen tissue repair[18,19]. MSCs can be administered locally or systemically, in which local administration has an advantage that MSCs can directly reach the lesion site (target organ), also known as non-systemic homing[20]. In the case of intravenous administration, however, MSCs are easy to be trapped in the lung, liver or spleen because they are bigger, and the expression of adhesion molecules [such as integrins cluster of differentiation (CD) 49 or CD49d] will reduce the number of cells delivered to the target site (about 2%)[21]. The effective homing and migration toward the lesion site of MSCs play vital roles in the treatment with MSCs. This study aims to determine whether the treatment with MSCs can improve the recovery of limb function to ameliorate peripheral nerve injury, and to further explore the underlying mechanism.

Materials and Methods

Materials

Big-ear rabbits (Laboratory Animal Research Center of the Hospital), bicinchoninic acid assay (BCA; Beyotime Biotechnology, Beijing, China), radio immunoprecipitation assay (RIPA; Applygen, Beijing, China), Leitz 1516 tissue microtome (Leica, Wetzlar, Germany), electromyogram instrument (Medtronic Keypoint, Minneapolis, MN, USA), electronic balance (Eppendorf, Hamburg, Germany), and primary antibodies of phosphorylated mitogen-activated protein kinase (p-MAP) and phosphorylated extracellular signal-regulated kinase (p-ERK; Abcam, Cambridge, MA, USA).

Objects and Grouping

Red fluorescent protein (RFP)-bone marrow MSCs (BMSCs) were divided into RFP-vector-BMSCs group and RFP-BMSCs group during construction based on varying transfection reagents. The objects big-ear rabbits were assigned into sham-operation group (Sham group, n=15), model + normal saline group (Model group, n=15), and model + RFP-BMSCs group (Treat group, n=15). This investigation was approved by the Animal Ethics Committee of Zhengzhou University Animal Center.

Separation and Purification of Rabbit BMSCs

The rabbits were anesthetized by midazolam (0.2-2.0 mg/kg), and the knees were cleansed using soap and scrubbed with povidone-iodine (PVP-I). Then, 8.0 mL of bone marrow at the proximal tibia was harvested by virtue of an aspiration needle and a 12 mL syringe containing 2.0 mL of heparin sodium injection. The heparinized bone marrow was washed with phosphate-buffered saline (PBS) and then centrifuged at 1500 rpm and room temperature for 5 min. After that, the layer of nucleated cells was resuspended in a Dulbecco's Modified Eagle's medium (DMEM) containing 10% fetal bovine serum (FBS) and 1% antibiotics, and the cells were seeded in a 100 cm^2 plate, incubated under culture conditions of adherent cells, and washed using PBS three days later. Next, the medium was replaced, and the purified cells were digested with trypsin when the cell fusion reached over 70%.

Rabbit Model of Brachial Plexus Root Avulsion Injury (BPAI)

The BPAI model was established under the anesthesia by intraperitoneal injection of 10% chloral hydrate. For the convenience of operation, the rabbits were placed in the prone position. An incision was made from the back of the neck along the midline of the body under the sterile conditions. The process of thoracic vertebra 2 was discov-

ered, and the left muscles were separated to expose the facets of vertebrae C4-T1. Subsequently, hemi-laminectomy was performed for left C4-T1 using micro-dissecting scissors, so as to expose the dorsal roots of C5-T1. Thereafter, the dorsal roots of C5-T1 were torn off from the spinal cord to expose the ventral roots, which were avulsed *via* the same methods. The operation was conducted under an operating microscope. Sham group received semi-blind resection of left C4-T1 and exposure of brachial plexuses (C5, C6, C7, C8, and T1), and then the incision was closed, without tearing the brachial plexuses.

Recovery Rate of Wet Weight of Upper Limb Muscle

The upper limb muscle tissues of the rabbits anesthetized and sacrificed 3 weeks later were taken, and intact triceps muscle was dissected from the origins and terminations of the upper limb. Next, the tissues were cleaned with PBS to remove the residual bloodstains and fragments on the tissues, followed by natural drying. The triceps muscles of both arms were weighed using the electronic balance, and the muscle recovery rate was calculated according to the following formula, so as to evaluate the changes in functional restoration of impaired tissues.

Formula: recovery rate of wet weight = wet weight of upper limb muscle on the operation side/ wet weight of upper limb muscle on the healthy side ×100%.

Hematoxylin and Eosin (HE) Staining for Nerve Tissues

The aforementioned muscle tissues were taken, a portion of which was quickly frozen in liquid nitrogen to prepare frozen sections, and the other portion was fixed for 24 h, embedded in paraffin and sliced to 1.5 μm-thick sections through the microtome, followed by HE staining. For the purpose of more thorough deparaffinization, the sections were put in an oven at 65°C the day before experiment, then deparaffinized and dehydrated at the beginning of the experiment, stained with hematoxylin for 4 min, flushed in running water for 1 min and counterstained with eosin for 1 min, followed by dehydration, clearing, mounting, and observation of results.

Electrophysiological Examination

Electrophysiological examination was performed on the injured side immediately before killing the rabbits, where the dorsal roots of C5-T1 were exposed after anesthesia of the rabbits. Then stimulating electrodes were placed above and below the injured segments, while recording electrodes were put in the upper limb muscles, and amplitude and latency of compound muscle action potential (CMAP) were recorded by the electromyogram instrument, which were mainly used to evaluate the recovery of muscle function after neural injury.

Transfection of RFP Label into BMSCs

The third-generation BMSCs obtained through separation and purification were inoculated into a 12-well plate, RFP transfection reagent was taken out and thawed on ice, and 100 μL of RFP reagent and 400 μL of enhancing fluid were added into the cells in accordance with the transfection instructions, which were replaced with a complete medium 6 h later, followed by culture for 12 h. Finally, the intensity of red fluorescence was observed under a fluorescence microscope, and if it met the requirements, the cells would be continuously cultured to obtain the stably expressed RFP-BMSCs.

Western Blotting

After the rabbits were anesthetized and sacrificed, the nerve tissues were taken out and resuspended in a mixture of cold RIPA cell lysate and protease inhibitor, followed by ultrasonication at 100 w for 5 s × 3 times. The absorbance at 560 nm was detected to calculate the protein concentration, and the samples were isolated *via* polyacrylamide gel and then transferred to membranes under constant current (300 mA) to block non-specific sites for 1 h, followed by incubation with primary antibodies for 16 h and with secondary antibodies for 1 h, image development and preservation of experimental results.

Statistical Analysis

Statistical Product and Service Solutions (SPSS) 17.0 (SPSS Inc., Chicago, IL, USA) software was employed to record the experimental results obtained, and *t*-test and univariate analysis were used as statistical methods, in which $p<0.05$ suggested statistically significant differences.

Results

Flow Cytometry Sorting of Purified BMSCs

The $CD45^-$ and $CD90^+$ BMSCs were sorted out *via* flow cytometry based on markers ($CD45^-$ and $CD90^+$) on the surface of BMSCs (Figure 1).

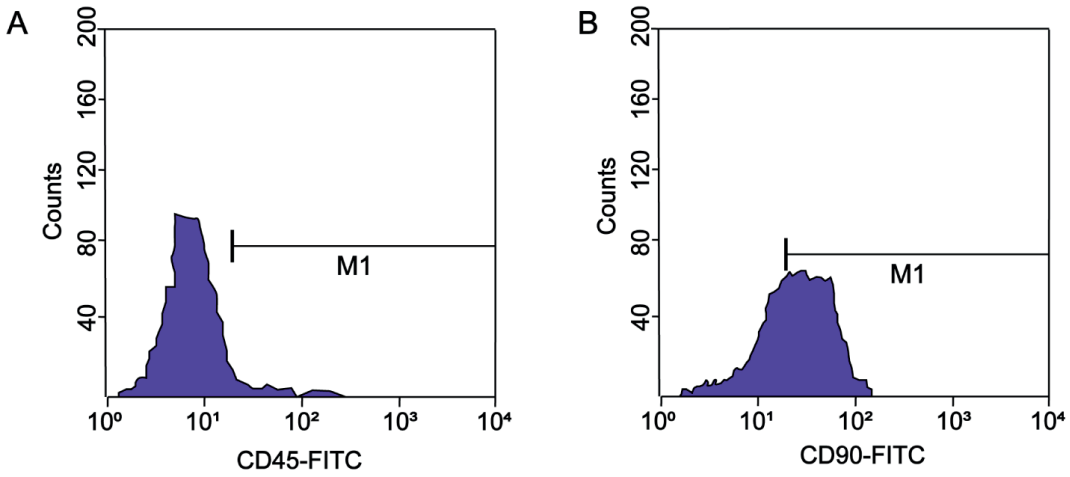

Figure 1. CD45$^-$ and CD90$^+$ BMSCs sorted out *via* flow cytometry. **A,** CD45$^-$, **B,** CD90$^+$.

Expression of Red Fluorescence Observed in RFP-BMSCs

At 12 h after transfection, the expression intensity of red fluorescence was observed under the fluorescence microscope (Figure 2).

Recovery Rate of Wet Muscle Weight

Compared with Sham group, Model group had a remarkably decreased recovery rate of wet muscle weight ($p<0.05$), while Treat group exhibited a notably increased recovery rate of wet muscle weight in comparison with Model group ($p<0.05$; Figure 3).

Pathological Changes in Impaired Nerve Tissue Sections

In Sham group, there was massive close packing, large myelinated fibers, and endoneurial vessels. In Model group, the characteristics of neural injury were present, the axons and large myelinated fibers were decreased, the density of nerve fibers was reduced, the axonal degeneration was increased, and the pathological phenomena such as axonal atrophy occurred. Similar morphology to that in Sham group was observed in Treat group, the number of axons and myelinated fibers was increased, the density of nerve fibers was raised,

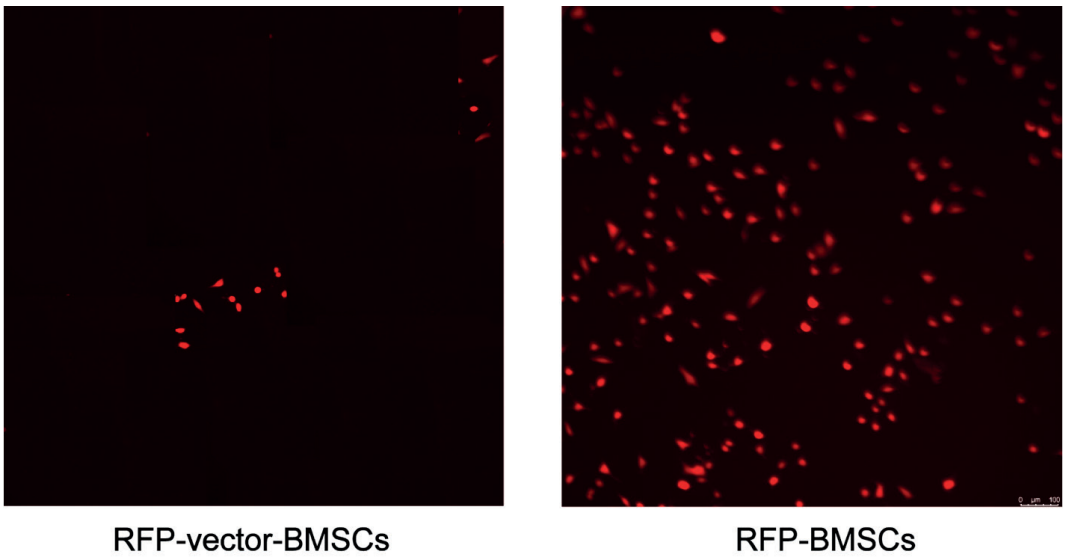

Figure 2. Expression intensity of red fluorescence at 12 h after transfection (Left: the transfection efficiency of empty plasmid fluorescence is lower than 5%. Right: the fluorescence intensity of transfected RFP is greater than 70%) (magnification: 200×).

Table I. Changes in CMAP.

	Sham group	Model group	Treat group	p (*)	p (#)
Amplitude (mv)	32±0.54	15.50±2.1	28±1.25	0.046	0.035
Latency (ms)	1.32±0.56	3.54±0.31	2.07±0.24	0.004	0.045

and the number of axonal regeneration and the axonal degeneration were decreased (Figure 4).

Electrophysiological Examination of Impaired Nerves

The CMAP amplitude was reduced markedly (p<0.05), while the CMAP latency was prolonged significantly (p<0.05) in Model group compared with those in Sham group. Moreover, Treat group displayed distinctly higher CMAP amplitude (p<0.05) and evidently shorter CMAP latency (p<0.05) than Model group (Table I and Figure 5).

RFP-BMSCs Traced in Impaired Nerve Tissues

The frozen sections were observed under the fluorescence microscope, and it was discovered that RFP-BMSCs were distributed along the nerve fibers in Treat group, indicating that RFP-BMSCs migrated to the site of nerve tissue injury (Figure 6).

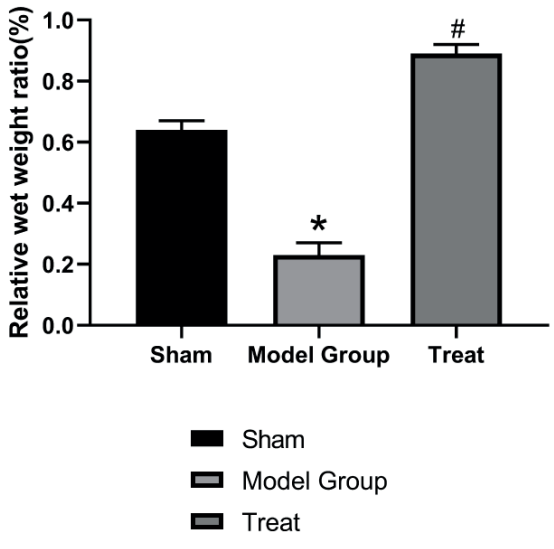

Figure 3. Statistical chart of recovery rate of wet muscle weight. *: Compared with Sham group, Model group has a remarkably decreased recovery rate of wet muscle weight, #: Treat group exhibits a notably increased recovery rate of wet muscle weight in comparison with Model group (*p<0.05, #p<0.05).

Changes in the MAPK/ERK Pathway in Impaired Nerve Tissues

The levels of p-MAPK and p-ERK were remarkably elevated in Model group in comparison with those in Sham group (p<0.05), while they were clearly lowered in Treat group compared with those in Model group (p<0.05; Figure 7).

Discussion

The problem of structural and functional reconstruction of peripheral nerve deficit has not been solved in clinical practices yet, especially the widespread injury of synaptic cleft[2]. With the development of nerve tissue engineering, the micro-environment of regeneration can be optimized by combining with biomaterial scaffolds, seed cells, and growth-promoting factors[1,22-24]. The transplantation of seed cells is the key strategy of nerve tissue engineering, and it is believed that the transplanted cells play positive roles in improving the micro-environment of regenerated axons. Schwann cells are structural and functional cells in peripheral nerves, which are crucial players in neural regeneration and can promote the neural regeneration as transplanted seed cells *in vivo*. However, the limitation of Schwann cell donors, excess incidence of donor nerves, and ineffective cell proliferation attenuate the clinical utility of those cells[25,26]. BMSCs are attractive stem cells because they have such merits as easy acquisition, rapid proliferation, persistent survival, and immune compatibility. Besides, BMSCs can differentiate into various lineages and secret neurotrophic factors that facilitate nerve cell regeneration[27]. BMSCs have been applied to repair central and peripheral nerve injuries to some extent. Nerve scaffolds provide structural support for sprouting neurites, and they have been utilized to bridge peripheral nerve defects[28]. In addition, the anti-apoptotic factor and vascular endothelial growth factor secreted by BMSC can protect the nerve injury. After the central nervous system injury, the apoptosis of the cells in the injured site will be induced. Bcl-2 can regulate injury-in-

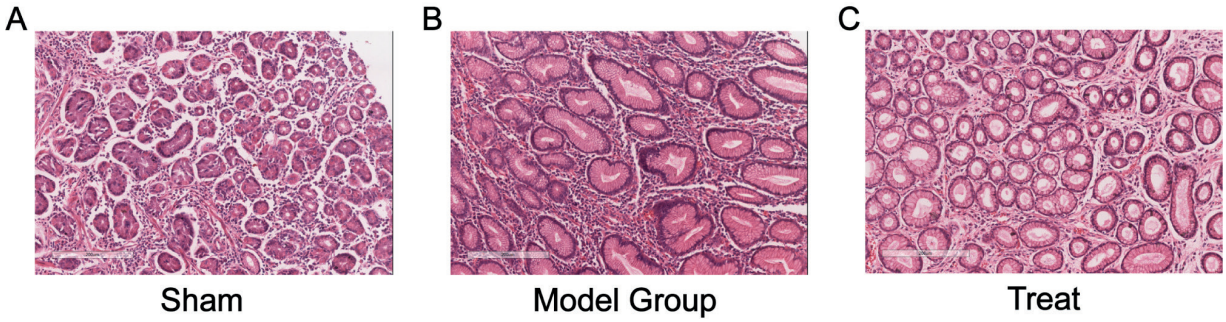

Figure 4. Pathological changes in impaired nerve tissue sections. **A,** In Sham group, there is massive close packing, large myelinated fibers and endoneurial vessels. **B,** In Model group, the axons and nerve fiber density are reduced, and the axonal degeneration is increased. **C,** Compared with Model group, Treat group has increased number of axons and density of myelinated fibers and nerve fibers (magnification: 400×).

duced apoptosis and effectively protects injured local neurons. VEGF is widely known for its role as an endothelial cell growth factor. Neurons also express their receptors of VEGF. VEGF prolongs the lifespan of cultured brain neurons and protects hippocampal and cortical neurons from serum deficiency, hypoxia, and glutamate-induced cell death[29,30].

The present study primarily aims to investigate the role of BMSCs in repairing the brachial plexus injury and their correlation with the MAPK/ERK pathway. In addition to behavioral variations, neural injury more importantly affects the movements of innervated muscles and the changes in potential of nerve fibers. BMSCs were extracted from the bone marrow fluid of big-ear rabbits firstly, and then $CD45^-$ and $CD90^+$ BMSCs were sorted out *via* flow cytometry, purified, and cultured continuously to harvest the third-generation BMSCs. To facilitate the tracing of BMSCs, RFP was transfected into the BMSCs. RFP is stably expressed in almost all the cells, so it is widely used to trace markers in research. RFP-BMSCs were constructed by transfecting the RFP label and detecting the intensity and efficiency of red fluorescence at 12 h after transfection. Next, the rabbit model of BPAI was established and treated with intravenous injection of normal saline and RFP-BMSCs. The degree of muscle atrophy is usually closely associated with the recovery of neurological function, so the recovery rate of wet muscle weight was applied to reflect the degree of muscle contraction. The determination of recovery rate of wet weight of upper limb muscle in Sham group, Model group, and Treat group revealed that the recovery rate of wet muscle weight declined remarkably in Model group compared with that in Sham group, while it rose evidently in Treat group in comparison with that in Model group, suggesting that injecting BMSCs into

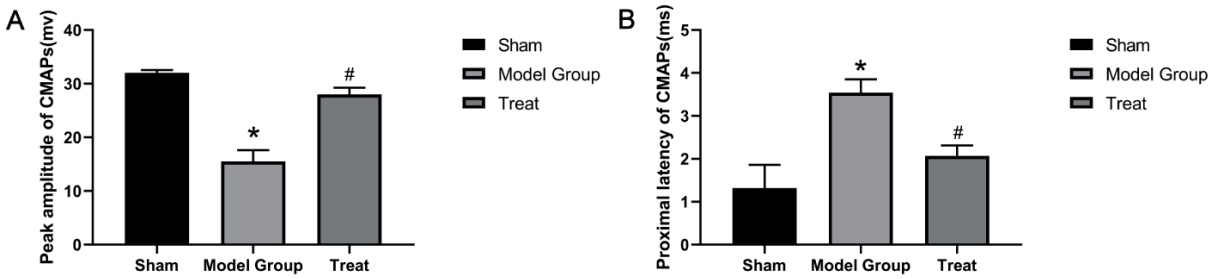

Figure 5. Electrophysiological examination of impaired nerve tissues. **A,** CMAP amplitude is reduced markedly in Model group compared with that in Sham group ($p<0.05$). #: The CMAP amplitude is raised distinctly in Treat group compared with that in Model group ($p<0.05$). **B,** CMAP latency is also extended notably in Model group in comparison with that in Sham group ($p<0.05$). #: The CMAP latency it is shortened significantly in Treat group in comparison with that in Model group ($p<0.05$) (*$p<0.05$, #$p<0.05$).

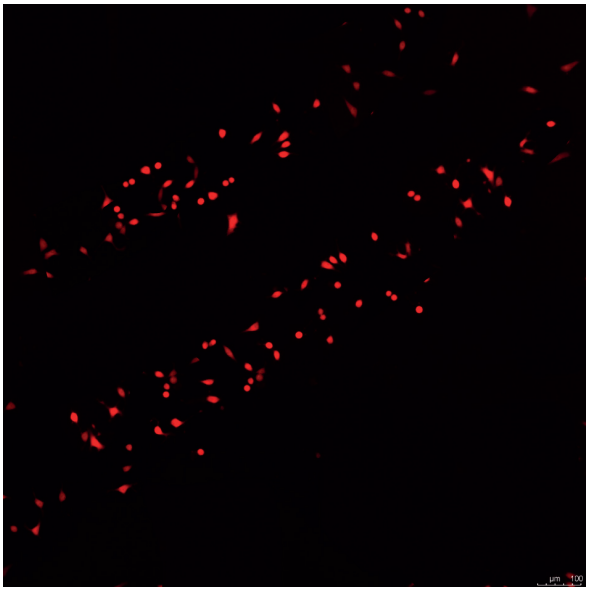

Figure 6. Distribution of RFP-BMSCs observed under fluorescence microscope (magnification: 200×).

rabbits can restore the contractibility of muscle tissues on the operated side. According to the HE staining of nerve tissue sections, Sham group exhibited a large amount of close packing, large myelinated fibers, and endoneurial vessels. The characteristics of neural injury, decreased axons, large myelinated fibers, and nerve fiber density, increased axonal degeneration, atrophy of axon, and other pathological phenomena were detected in Model group. In Treat group, similar morphology to that in Sham group was observed, the number of axons and the density of myelinated fibers and nerve fibers were raised remarkably, and the number of axonal regenerations was reduced. The nerve fibers also have a vital function of conducting excitation. It was observed through the electromyogram instrument that compared with those in Sham group, the CMAP amplitude was decreased markedly and the latency was extended notably in Model group. In comparison with Model group, Treat group had prominently elevated CMAP amplitude and shortened latency. Those experimental results manifested that the excitation conduction function of the impaired nerve fibers is recovered after the treatment with BMSCs. To further observe whether the BMSCs exert the nerve repairing effect, it was detected that large quantities of RFP-BMSCs aggregated at the injured nerves in the frozen pathological nerve sections, illustrating that the RFP-BMSCs injected intravenously migrate to the periphery of the injured nerves to exert their repairing effect. Many literature reports indicated that ERK is involved in the repair of neural injury. The protein expressions of p-ERK and p-MAPK in impaired nerve tissues were examined *via* Western blotting assay, so as to explore the correlation between the repair process of stem cells in nerves and ERK. The results showed that the expressions of p-ERK and p-MAPK were distinctly higher in Model group than those in Sham group, while they were markedly lower in Treat group than those in Model group, demonstrating that the MAPK/ERK pathway is implicated in the repairing of stem cells in neural injury. After experimental studies step by step, it was ultimately concluded that the BMSCs can repair the impaired brachial plexus,

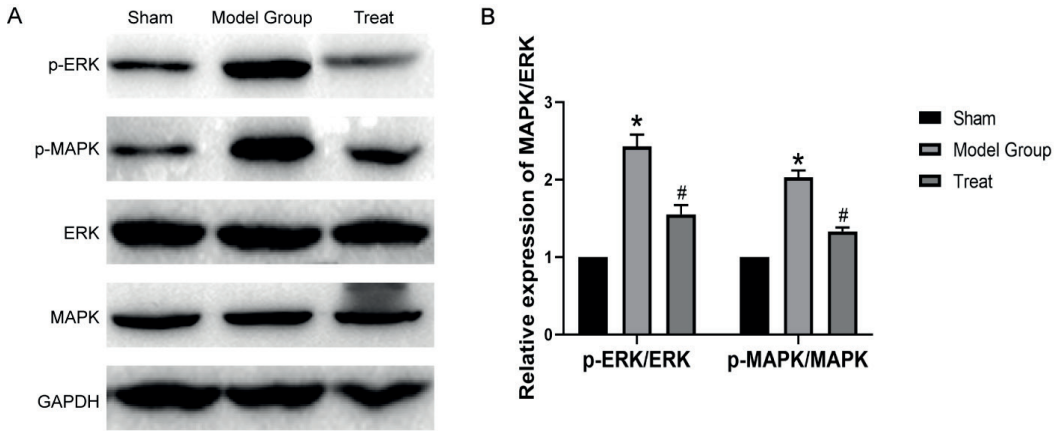

Figure 7. Changes in protein expressions of the MAPK/ERK pathway in impaired nerve tissues **A,** and **B,** Levels of p-MAPK and p-ERK are elevated remarkably in Model group in comparison with those in Sham group ($p<0.05$), and #: they are lowered clearly in Treat group in comparison with those in Model group ($p<0.05$) (*$p<0.05$, #$p<0.05$).

and such a process is related to the MAPK/ERK pathway. This research is of favorable guiding significance for the treatment of brachial plexus injury, but the demerits of low concentration of BMSCs *in vivo* and great difficulty of purification need to be solved in the future.

Conclusions

The present study showed that BMSCs can repair the impaired brachial plexus neurons and restore their physiological functions, and the protective effect of the BMSCs on the neurons is associated with the mediated MAPK/ERK pathway.

Conflicts of interest

The authors declare no conflicts of interest.

References

1) Noble J, Munro CA, Prasad VS, Midha R. Analysis of upper and lower extremity peripheral nerve injuries in a population of patients with multiple injuries. J Trauma 1998; 45: 116-122.
2) DeHart MM, Riley LJ. Nerve injuries in total hip arthroplasty. J Am Acad Orthop Surg 1999; 7: 101-111.
3) Gu S, Shen Y, Xu W, Xu L, Li X, Zhou G, Gu Y, Xu J. Application of fetal neural stem cells transplantation in delaying denervated muscle atrophy in rats with peripheral nerve injury. Microsurg 2010; 30: 266-274.
4) Dadon-Nachum M, Melamed E, Offen D. Stem cells treatment for sciatic nerve injury. Expert Opin Biol Ther 2011; 11: 1591-1597.
5) Rochkind S, Geuna S, Shainberg A. Chapter 25: phototherapy in peripheral nerve injury: effects on muscle preservation and nerve regeneration. Int Rev Neurobiol 2009; 87: 445-464.
6) Pan HC, Cheng FC, Chen CJ, Lai SZ, Lee CW, Yang DY, Chang MH, Ho SP. Post-injury regeneration in rat sciatic nerve facilitated by neurotrophic factors secreted by amniotic fluid mesenchymal stem cells. J Clin Neurosci 2007; 14: 1089-1098.
7) Goel RK, Suri V, Suri A, Sarkar C, Mohanty S, Sharma MC, Yadav PK, Srivastava A. Effect of bone marrow-derived mononuclear cells on nerve regeneration in the transection model of the rat sciatic nerve. J Clin Neurosci 2009; 16: 1211-1217.
8) Pan HC, Chen CJ, Cheng FC, Ho SP, Liu MJ, Hwang SM, Chang MH, Wang YC. Combination of G-CSF administration and human amniotic fluid mesenchymal stem cell transplantation promotes peripheral nerve regeneration. Neurochem Res 2009; 34: 518-527.
9) Chen L, Jin Y, Yang X, Liu Z, Wang Y, Wang G, Qi Z, Shen Z. Fat tissue, a potential Schwann cell reservoir: isolation and identification of adipose-derived Schwann cells. Am J Transl Res 2017; 9: 2579-2594.
10) Li M, Ikehara S. Bone-marrow-derived mesenchymal stem cells for organ repair. Stem Cells Int 2013; 2013: 132642.
11) Kitada M. Mesenchymal cell populations: development of the induction systems for Schwann cells and neuronal cells and finding the unique stem cell population. Anat Sci Int 2012; 87: 24-44.
12) Dezawa M, Takahashi I, Esaki M, Takano M, Sawada H. Sciatic nerve regeneration in rats induced by transplantation of in vitro differentiated bone-marrow stromal cells. Eur J Neurosci 2001; 14: 1771-1776.
13) Coronel MF, Musolino PL, Brumovsky PR, Hokfelt T, Villar MJ. Bone marrow stromal cells attenuate injury-induced changes in galanin, NPY and NPY Y1-receptor expression after a sciatic nerve constriction. Neuropeptides 2009; 43: 125-132.
14) Karussis D, Kassis I, Kurkalli BG, Slavin S. Immunomodulation and neuroprotection with mesenchymal bone marrow stem cells (MSCs): a proposed treatment for multiple sclerosis and other neuroimmunological/neurodegenerative diseases. J Neurol Sci 2008; 265: 131-135.
15) Tang Y, Yasuhara T, Hara K, Matsukawa N, Maki M, Yu G, Xu L, Hess DC, Borlongan CV. Transplantation of bone marrow-derived stem cells: a promising therapy for stroke. Cell Transplant 2007; 16: 159-169.
16) Volarevic V, Arsenijevic N, Lukic ML, Stojkovic M. Concise review: mesenchymal stem cell treatment of the complications of diabetes mellitus. Stem Cells 2011; 29: 5-10.
17) Zhu CJ, Dong JX, Zhang MJ, Lu GL, Li J. [Effect of acupoint injection with bone marrow mesenchymal stem cells on the blood flow in rats with hind limb ischemia]. Zhongguo Zhen Jiu 2009; 29: 987-992.
18) Gonzalez-Rey E, Gonzalez MA, Varela N, O'Valle F, Hernandez-Cortes P, Rico L, Buscher D, Delgado M. Human adipose-derived mesenchymal stem cells reduce inflammatory and T cell responses and induce regulatory T cells in vitro in rheumatoid arthritis. Ann Rheum Dis 2010; 69: 241-248.
19) Yoo KH, Jang IK, Lee MW, Kim HE, Yang MS, Eom Y, Lee JE, Kim YJ, Yang SK, Jung HL, Sung KW, Kim CW, Koo HH. Comparison of immunomodulatory properties of mesenchymal stem cells derived from adult human tissues. Cell Immunol 2009; 259: 150-156.
20) Ra JC, Shin IS, Kim SH, Kang SK, Kang BC, Lee HY, Kim YJ, Jo JY, Yoon EJ, Choi HJ, Kwon E. Safety of intravenous infusion of human adipose tissue-derived mesenchymal stem cells in animals and humans. Stem Cells Dev 2011; 20: 1297-1308.
21) Nystedt J, Anderson H, Tikkanen J, Pietila M, Hirvonen T, Takalo R, Heiskanen A, Satomaa T, Natunen S, Lehtonen S, Hakkarainen T, Korhonen M, Laitinen S, Valmu L, Lehenkari P. Cell surface structures influence lung clearance rate of systemically infused mesenchymal stromal cells. Stem Cells 2013; 31: 317-326.

22) Ao Q, Fung CK, Tsui AY, Cai S, Zuo HC, Chan YS, Shum DK. The regeneration of transected sciatic nerves of adult rats using chitosan nerve conduits seeded with bone marrow stromal cell-derived Schwann cells. Biomaterials 2011; 32: 787-796.

23) Ciardelli G, Chiono V. Materials for peripheral nerve regeneration. Macromol Biosci 2006; 6: 13-26.

24) Crouzier T, McClendon T, Tosun Z, McFetridge PS. Inverted human umbilical arteries with tunable wall thicknesses for nerve regeneration. J Biomed Mater Res a 2009; 89: 818-828.

25) Mosahebi A, Fuller P, Wiberg M, Terenghi G. Effect of allogeneic Schwann cell transplantation on peripheral nerve regeneration. Exp Neurol 2002; 173: 213-223.

26) Wang Y, Li WY, Jia H, Zhai FG, Qu WR, Cheng YX, Liu YC, Deng LX, Guo SF, Jin ZS. KLF7-transfected Schwann cell graft transplantation promotes sciatic nerve regeneration. Neuroscience 2017; 340: 319-332.

27) Yang X, Chen J, Xue P, Liu R, Ji W, Lu X, Liu X, Chen Z. Differentiation of bone marrow stromal cells into schwann-like cells using dihydrotestosterone combined with a classical induction method. Biotechnol Lett 2017; 39: 331-337.

28) Cuevas P, Carceller F, Garcia-Gomez I, Yan M, Dujovny M. Bone marrow stromal cell implantation for peripheral nerve repair. Neurol Res 2004; 26: 230-232.

29) Le Bras B, Barallobre MJ, Homman-Ludiye J, Ny A, Wyns S, Tammela T, Haiko P, Karkkainen MJ, Yuan L, Muriel MP, Chatzopoulou E, Breant C, Zalc B, Carmeliet P, Alitalo K, Eichmann A, Thomas JL. VEGF-C is a trophic factor for neural progenitors in the vertebrate embryonic brain. Nat Neurosci 2006; 9: 340-348.

30) Jin KL, Mao XO, Greenberg DA. Vascular endothelial growth factor: direct neuroprotective effect in in vitro ischemia. Proc Natl Acad Sci U S A 2000; 97: 10242-10247.